

2 Bonds

2.1 Introduction

The positively charged atomic nuclei and the electrons in the atomic shells of the atoms making up the semiconductor (or any other solid) are in a binding state. Several mechanisms can lead to such cohesiveness. First, we will discuss the homopolar, electron-pair or covalent bond, then the ionic bond and subsequently the mixed bond. We will only briefly touch on the metallic bond and the van-der-Waals bond.

2.2 Covalent Bonds

Covalent bonds are formed due to quantum-mechanical forces. The prototype covalent bond is the bonding of the hydrogen molecule due to overlapping of the atomic shells. If several electron pairs are involved, directional bonds can be formed in various spatial directions, eventually making up a solid.

2.2.1 Electron-Pair Bond

The covalent bond of two hydrogen atoms in a H_2 molecule can lead to a reduction of the total energy of the system, compared to two single (distant) atoms (Fig. 2.1). For fermions (electrons have spin 1/2) the two-particle wavefunction of the two (indistinguishable) electrons A and B must be antisymmetric, i.e. $\Psi(A, B) = -\Psi(B, A)$ (Pauli principle). The wavefunction of each electron has degrees of freedom in real space (\mathbf{r}) and spin (σ), $\Psi(A) = \Psi_{\mathbf{r}}(A)\Psi_{\sigma}(A)$. The two-particle wavefunction of the molecule is non-separable and has the form $\Psi(A, B) = \Psi_{\mathbf{r}}(r_A, r_B)\Psi_{\sigma}(\sigma_A, \sigma_B)$. The binding state has a wavefunction with a symmetric orbital and antiparallel spins, i.e. $\Psi_{\mathbf{r}}(r_A, r_B) = \Psi_{\mathbf{r}}(r_B, r_A)$ and $\Psi_{\sigma}(\sigma_A, \sigma_B) = -\Psi_{\sigma}(\sigma_B, \sigma_A)$. The antisymmetric orbital with parallel spins is antibinding for all distances of the nuclei (protons).

2.2.2 sp^3 Bonds

Elements from group IV of the periodic system (C, Si, Ge, ...) have 4 electrons on the outer shell. Carbon has the electron configuration $1s^2 2s^2 2p^2$.

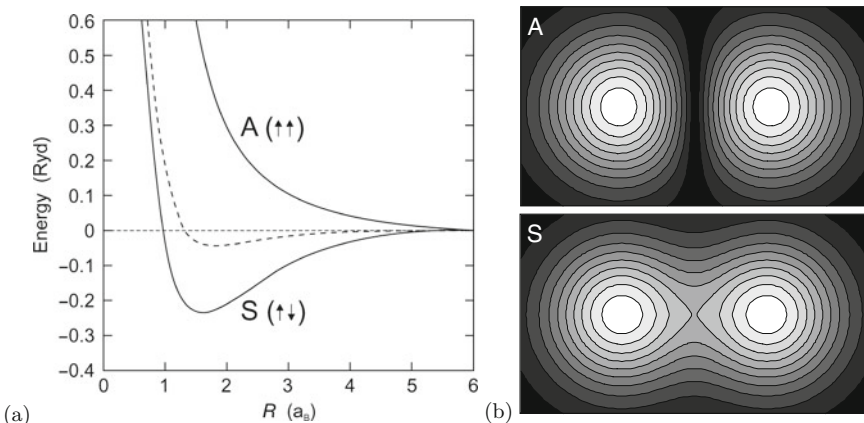


Fig. 2.1. Binding of the hydrogen molecule. (a) Dashed line: classical calculation (electrostatics), ‘S’, ‘A’: quantum-mechanical calculation taking into account Pauli’s principle (S: symmetric orbital, antiparallel spins, A: antisymmetric orbital, parallel spins). The distance of the nuclei (protons) is given in units of the Bohr radius $a_B = 0.053$ nm, the energy is given in Rydberg units (13.6 eV). (b) Schematic contour plots of the probability distribution ($\Psi^*\Psi$) for the S and A states

For an octet configuration bonding to four other electrons would be optimal (Fig. 2.2). This occurs through the mechanism of sp^3 hybridization.¹ First, one electron of the ns^2np^2 configuration is brought into a p orbital, such that

DIE WUNDERSAME WELT DER ATOMIS

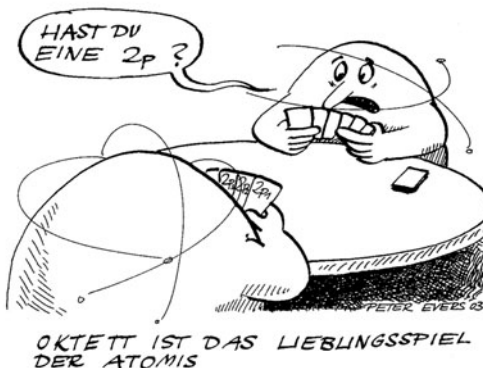


Fig. 2.2. Octet, the favorite card game of the ‘Atomis’ (trying to reach octet configuration in a bond by swapping wavefunctions). The bubble says: ‘Do you have a 2p?’ Reprinted with permission from [99], ©2002 Wiley-VCH

¹It is debated in femtosecond chemistry whether the bond *really* forms in this way. However, it is a picture of overwhelming simplicity.

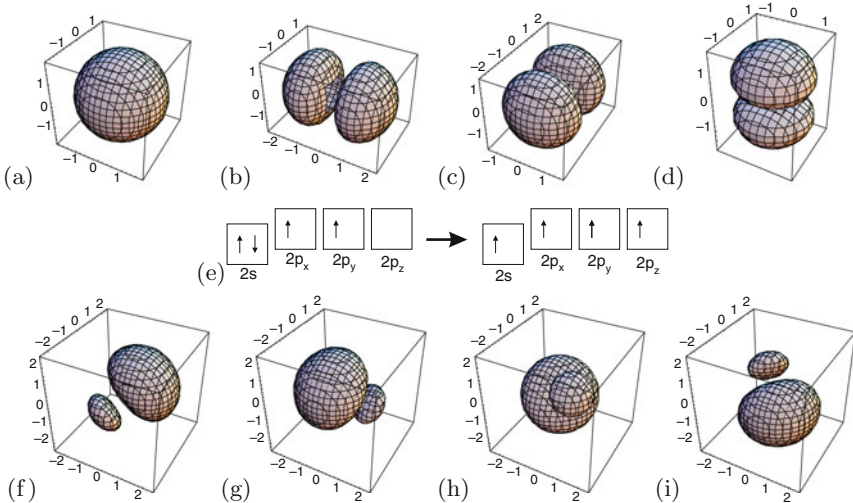


Fig. 2.3. (a) s orbital, (b,c,d) p_x, p_y and p_z orbital, (e) hybridization, (f,g,h,i) orbitals of the sp³ hybridization: (f) (s+p_x+p_y+p_z)/2, (g) (s+p_x-p_y-p_z)/2, (h) (s-p_x+p_y-p_z)/2, (i) (s-p_x-p_y+p_z)/2

the outermost shell contains one s, p_x, p_y, and p_z orbital each (Figs. 2.3a–e). The energy necessary for this step is more than regained in the subsequent formation of the covalent bonds. The four orbitals can be reconfigured into four other wavefunctions, the sp³ hybrids (Figs. 2.3f–i), i.e.

$$\Psi_{++++} = (s + p_x + p_y + p_z)/2 \quad (2.1a)$$

$$\Psi_{+---} = (s + p_x - p_y - p_z)/2 \quad (2.1b)$$

$$\Psi_{+-+-} = (s - p_x + p_y - p_z)/2 \quad (2.1c)$$

$$\Psi_{+-+-} = (s - p_x - p_y + p_z)/2. \quad (2.1d)$$

These orbitals have a directed form along tetrahedral directions. The binding energy (per atom) of the covalent bond is large, for H–H 4.5 eV, for C–C 3.6 eV, for Si–Si 1.8 eV, and for Ge–Ge 1.6 eV. Such energy is, for *neutral* atoms, comparable to the ionic bond, discussed in the next section.

In Fig. 2.4a the energy of a crystal made up from silicon atoms is shown for various crystal structures² or phases (cf. Chap. 3). We note that the crystal energy of further silicon structures are discussed in [98]). The lattice constant with the lowest total energy determines the lattice spacing for each crystal structure. The thermodynamically stable configuration is the phase with the lowest overall energy for given external conditions.

The covalent bond of a group-IV atom to other group-IV atoms has a tetrahedral configuration with electron-pair bonds, similar to the hydrogen molecule bond. In Fig. 2.4b the energy states of the n = 2 shell for

²Hexagonal diamond is wurtzite structure with two identical atoms in the base.

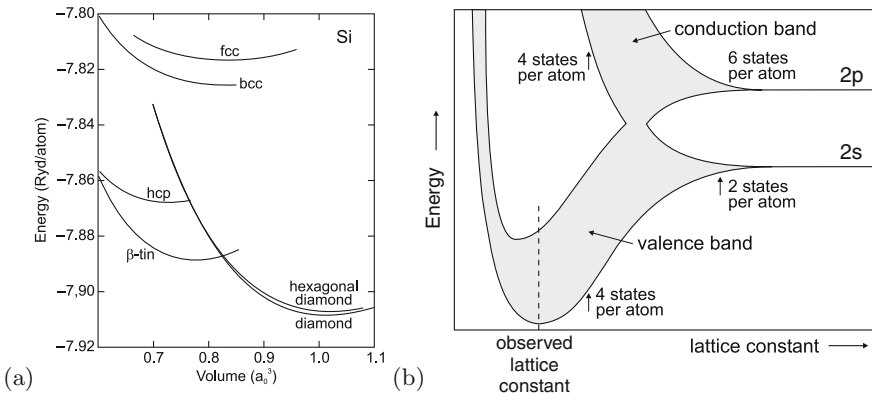


Fig. 2.4. (a) Energy per atom in silicon for various crystal structures. Adapted from [100]. (b) Electron energy levels in (diamond structure) carbon as a function of the distance of the atomic nuclei (schematic). Adapted from [101, 102]

tetrahedrally bonded carbon (diamond, see Sect. 3.4.3) are shown as a function of the distance from the nuclei. First, the energetically sharp states become a band due to the overlap and coupling of the atomic wavefunctions (cf. Sect. 6). The mixing of the states leads to the formation of the filled lower valence band (binding states) and the empty upper conduction band (antibinding states). This principle is valid for most semiconductors and is shown schematically also in Fig. 2.5. The configuration of bonding and antibonding p orbitals is depicted schematically in Fig. 2.6. The bonding and antibonding sp^3 orbitals are depicted in Figs. 2.7a,b and 2.13. We note that the energy of the crystal does not only depend on the distance from the nuclei but also on their geometric arrangement (crystal structure).

Per carbon atom there are (in the second shell) four electrons and four unoccupied states, altogether eight. These are redistributed into four states (filled) per atoms in the valence band and four states per atom (empty) in the conduction band. Between the top of the valence band and the bottom of the conduction band there is an energy gap, later called the *band gap* (cf. Chap. 6).

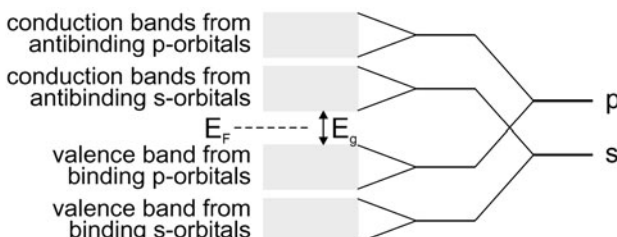


Fig. 2.5. Schematic of the origin of valence and conduction band from the atomic s and p orbitals. The band gap E_g and the position of the Fermi level E_F are indicated

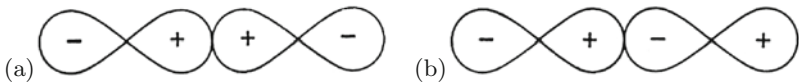


Fig. 2.6. Schematic representation of (a) bonding and (b) antibinding p orbitals. The *signs* denote the phase of the wavefunction

2.2.3 sp^2 Bonds

Organic semiconductors (see Chap. 16) are made up from carbon compounds. While for inorganic semiconductors the covalent (or mixed, cf. Sect. 2.4) bond with sp^3 hybridization is important, the organic compounds are based on the sp^2 hybridization. This bonding mechanism, which is present in graphite, is stronger than the sp^3 -bond present in diamond. The prototype organic molecule is the benzene ring³ (C_6H_6), shown in Fig. 2.8. The benzene ring is the building block for small organic molecules and polymers.

In the benzene molecule neighboring carbon atoms are bonded within the ring plane via the binding σ states of the sp^2 orbitals (Fig. 2.8a). The wavefunctions (Fig. 2.9) are given by (2.2a–c).

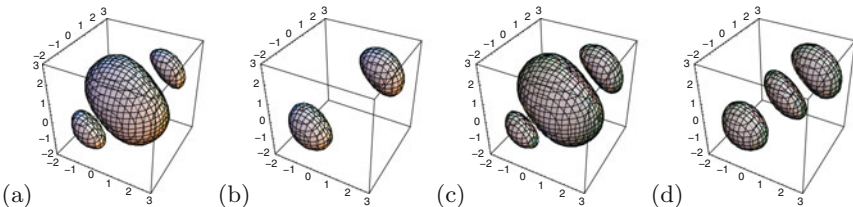


Fig. 2.7. Schematic representation of (a,c) bonding and (b,d) antibinding symmetric (a,b) and nonsymmetric (c,d) sp^3 orbitals

³Supposedly, the chemist Friedrich August Kekulé von Stadenitz had a dream about dancing carbon molecules and thus came up with the ring-like molecule structure [103]. Kekulé remembered: ‘During my stay in Ghent, I lived in elegant bachelor quarters in the main thoroughfare. My study, however, faced a narrow side-alley and no daylight penetrated it.... I was sitting writing on my textbook, but the work did not progress; my thoughts were elsewhere. I turned my chair to the fire and dozed. Again the atoms were gamboling before my eyes. This time the smaller groups kept modestly in the background. My mental eye, rendered more acute by the repeated visions of the kind, could now distinguish larger structures of manifold conformation; long rows sometimes more closely fitted together all twining and twisting in snake-like motion. But look! What was that? One of the snakes had seized hold of its own tail, and the form whirled mockingly before my eyes. As if by a flash of lightning I awoke; and this time also I spent the rest of the night in working out the consequences of the hypothesis.’

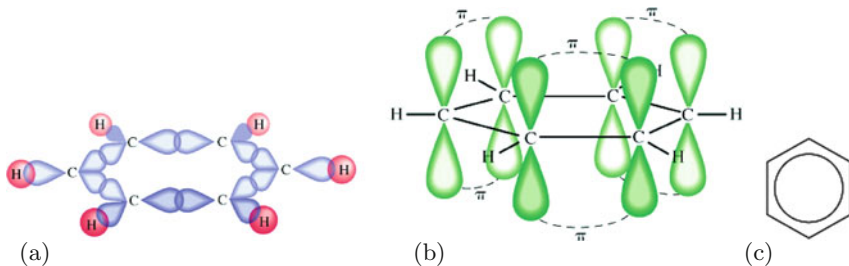


Fig. 2.8. Schematic representation of the (a) σ and (b) π bonds in benzene, (c) schematic symbol for benzene

$$\Psi_1 = (s + \sqrt{2} p_x)/\sqrt{3} \quad (2.2a)$$

$$\Psi_2 = (s - \sqrt{1/2} p_x + \sqrt{3/2} p_y)/\sqrt{3} \quad (2.2b)$$

$$\Psi_3 = (s - \sqrt{1/2} p_x - \sqrt{3/2} p_y)/\sqrt{3}. \quad (2.2c)$$

The ‘remaining’ p_z orbitals do not directly take part in the binding (Fig. 2.8b) and form bonding (π , filled) and antibonding (π^* , empty) orbitals (see Fig. 2.10). The π and π^* states are delocalized over the ring. Between the highest populated molecular orbital (HOMO) and the lowest unoccupied molecular orbital (LUMO) is typically an energy gap (Fig. 2.11). The antibinding σ^* orbitals are energetically above the π^* states.

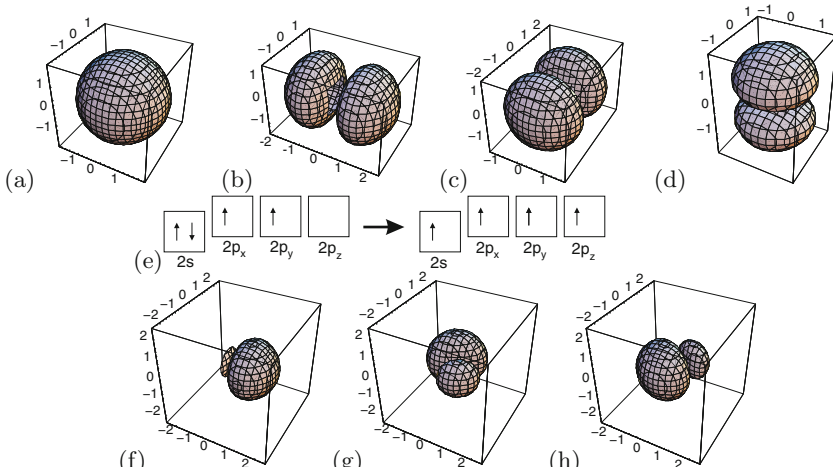


Fig. 2.9. (a) s orbital, (b,c,d) p_x, p_y and p_z orbital, (e) hybridization, (f,g,h) orbitals of the sp² hybridization: (f) $(s + \sqrt{2} p_x)/\sqrt{3}$, (g) $(s - \sqrt{1/2} p_x + \sqrt{3/2} p_y)/\sqrt{3}$, (h) $(s - \sqrt{1/2} p_x - \sqrt{3/2} p_y)/\sqrt{3}$

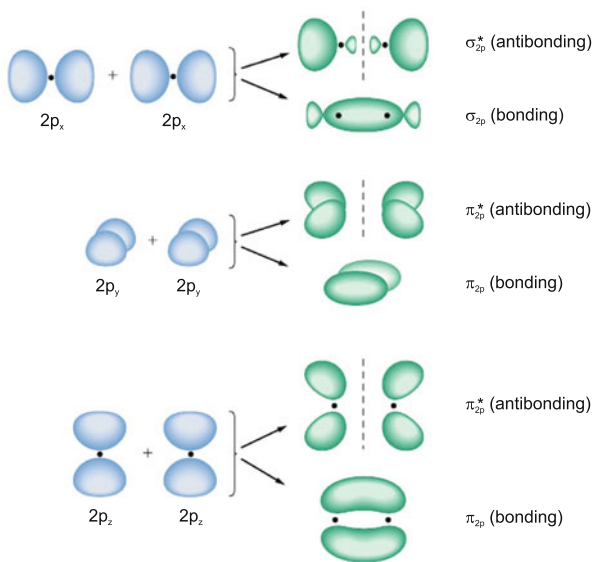


Fig. 2.10. Orbitals due to binding and antibinding configurations of various π orbitals

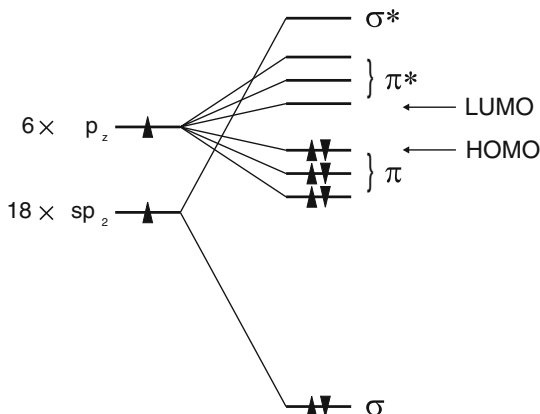


Fig. 2.11. Schematic energy terms of the benzene molecule

2.3 Ionic Bonds

Ionic crystals are made up from positively and negatively charged ions. The heteropolar or ionic bond is the consequence of the electrostatic attraction between the ions. However, the possibly repulsive character of next neighbors has to be considered.

For I–VII compounds, e.g. LiF or NaCl, the shells of the singly charged ions are complete: Li: $1s^2 2s^1 \rightarrow Li^+$; F: $1s^2 2s^2 2p^5 \rightarrow F^-$; $1s^2 2s^2 2p^6$.

Compared to ions in a gas, a Na–Cl pair in the crystal has a binding energy of 7.9 eV that mostly stems from the electrostatic energy (Madelung energy). Van-der-Waals forces (cf. Sect. 2.6) only contribute 1–2%. The ionization energy of Na is 5.14 eV, the electron affinity of Cl is 3.61 eV. Thus the energy of the NaCl pair in the solid is 6.4 (=7.9–5.1+3.6) eV smaller than in a gas of neutral atoms.

The interaction of two ions with distance vector \mathbf{r}_{ij} is due to the Coulomb interaction

$$U_{ij}^C = \frac{q_i q_j}{4\pi\epsilon_0} \frac{1}{r_{ij}} = \pm \frac{e^2}{4\pi\epsilon_0} \frac{1}{r_{ij}} \quad (2.3)$$

and a repulsive contribution due to the overlap of (complete) shells. This contribution is typically approximated by a radially symmetric core potential

$$U_{ij}^{\text{core}} = \lambda \exp(-\lambda/\rho) \quad (2.4)$$

that only acts on next neighbors. λ describes the strength of this interaction and ρ parameterizes its range.

The distance of ions is denoted as $r_{ij} = p_{ij}R$, where R denotes the distance of next neighbors and the p_{ij} are suitable coefficients. The electrostatic interaction of an ion with *all* its neighbors is then written as

$$U_{ij}^C = -\alpha \frac{e^2}{4\pi\epsilon_0} \frac{1}{R}, \quad (2.5)$$

where α is the Madelung constant. For an attractive interaction (as in a solid), α is positive. It is given (calculated for the i -th ion) as

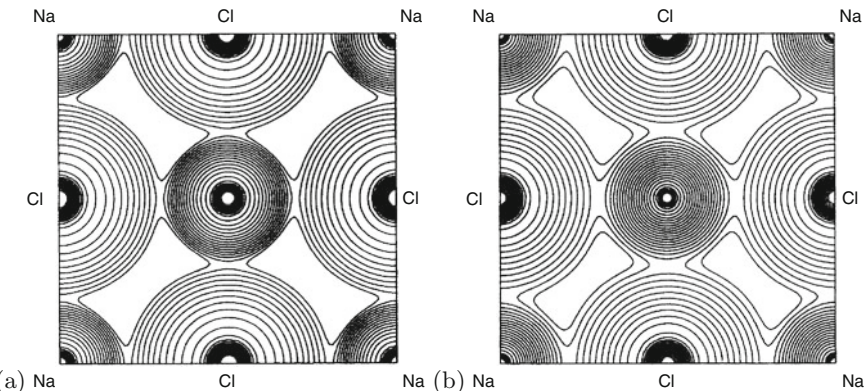


Fig. 2.12. (a) Experimental and (b) theoretical charge distribution in the (100) plane of NaCl. The lowest contour in the interstitial region corresponds to a charge density of 7 e/nm^3 and adjacent contours differ by $\sqrt{2}$. Differences are mainly due to the fact that the X-ray experiments have been made at room temperature. Adapted from [104]

$$\alpha = \sum_{ij} \frac{\pm 1}{p_{ij}}. \quad (2.6)$$

For a one-dimensional chain $\alpha = 2 \ln 2$. For the rocksalt (NaCl) structure (cf. Sect. 3.4.1) it is $\alpha \approx 1.7476$, for the CsCl structure (see Sect. 3.4.2) it is $\alpha \approx 1.7627$, and for the zincblende structure (see Sect. 3.4.4) it is $\alpha \approx 1.6381$. This shows that ionic compounds prefer the NaCl or CsCl structure. The charge distribution for NaCl is shown in Fig. 2.12. For tetragonal and orthorhombic structures, the Madelung constant has been calculated in [105].

2.4 Mixed Bonds

The group-IV crystals are of perfectly covalent nature, the I–VII are almost exclusively ionically bonded. For III–V (e.g. GaAs, InP) and II–VI compounds (e.g. CdS, ZnO) we have a mixed case.

The (screened) Coulomb potentials of the A and B atoms (in the AB compound) shall be denoted V_A and V_B . The origin of the coordinate system is in the center of the A and B atom (i.e. for the zincblende structure (cf. Sect. 3.4.4) at $(1/8, 1/8, 1/8)a$). The valence electrons then see the potential

$$V_{\text{crystal}} = \sum_{\alpha} V_A(\mathbf{r} - \mathbf{r}_{\alpha}) + \sum_{\beta} V_B(\mathbf{r} - \mathbf{r}_{\beta}), \quad (2.7)$$

where the sum α (β) runs over all A (B) atoms. This potential can be split into a symmetric (V_c , covalent) and an antisymmetric (V_i , ionic) part (2.8b), i.e. $V_{\text{crystal}} = V_c + V_i$

$$V_c = \frac{1}{2} \left\{ \sum_{\alpha} V_A(\mathbf{r} - \mathbf{r}_{\alpha}) + \sum_{\alpha} V_B(\mathbf{r} - \mathbf{r}_{\alpha}) + \sum_{\beta} V_B(\mathbf{r} - \mathbf{r}_{\beta}) + \sum_{\beta} V_A(\mathbf{r} - \mathbf{r}_{\beta}) \right\} \quad (2.8a)$$

$$V_i = \frac{1}{2} \left\{ \sum_{\alpha} V_A(\mathbf{r} - \mathbf{r}_{\alpha}) - \sum_{\alpha} V_B(\mathbf{r} - \mathbf{r}_{\alpha}) + \sum_{\beta} V_B(\mathbf{r} - \mathbf{r}_{\beta}) - \sum_{\beta} V_A(\mathbf{r} - \mathbf{r}_{\beta}) \right\}. \quad (2.8b)$$

For homopolar bonds $V_i = 0$ and the splitting between bonding and antibonding states is E_h , which mainly depends on the bond length l_{AB} (and the related overlap of atomic wavefunctions). In a partially ionic bond the orbitals are not symmetric along $A-B$, but the center is shifted towards the more electronegative material (Figs. 2.7c,d and 2.13).

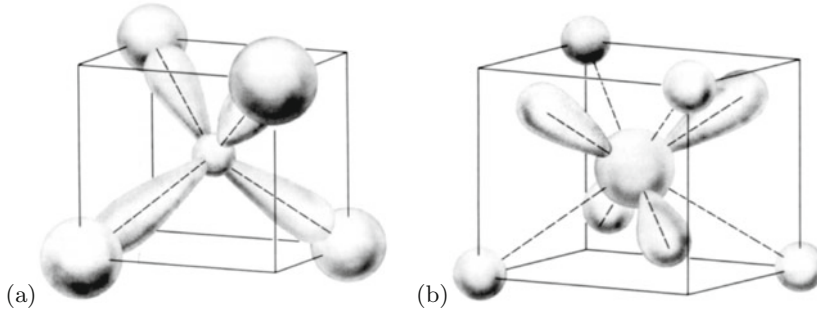


Fig. 2.13. Schematic representation of (a) bonding and (b) antibinding sp^3 orbitals. From [106]

The band splitting⁴ between the (highest) bonding and (lowest) antibinding state E_{ba} is then written as

$$E_{ba} = E_h + iC , \quad (2.9)$$

where C denotes the band splitting due to the ionic part of the potential and depends only on $V_A - V_B$. C is proportional to the difference of the electronegativities X of the A and B atoms, $C(A, B) = 5.75(X_A - X_B)$. A material thus takes a point in the (E_h, C) plane (Fig. 2.14). The absolute value for the band splitting is given as $E_{ba}^2 = E_h^2 + C^2$.

The ionicity of the bond is described with the ionicity (after Phillips) f_i , defined as [108]

$$f_i = \frac{C^2}{E_h^2 + C^2} . \quad (2.10)$$

The covalent part is $1 - f_i$. In Table 2.1 the ionicity is given for a number of binary compounds. The ionicity can also be interpreted as the angle $\tan(\phi) = C/E_h$ in the (E_h, C) diagram. The critical value of $f_i = 0.785$ for the ionicity separates quite exactly (for about 70 compounds) the 4-fold (diamond, zincblende and wurtzite) from the 6-fold (rocksalt) coordinated substances ($f_i = 0.785$ is indicated by a dashed line in Fig. 2.14).

For ionic compounds, an effective ionic charge e^* is defined connecting the displacement \mathbf{u} of negative and positive ions and the resulting polarization $\mathbf{P} = (e^*/2a^3) \mathbf{u}$ [109]. Connected with the ionicity is the so-called s -parameter, describing the change of the charge upon change of bond length b from its equilibrium value b_0 [110]

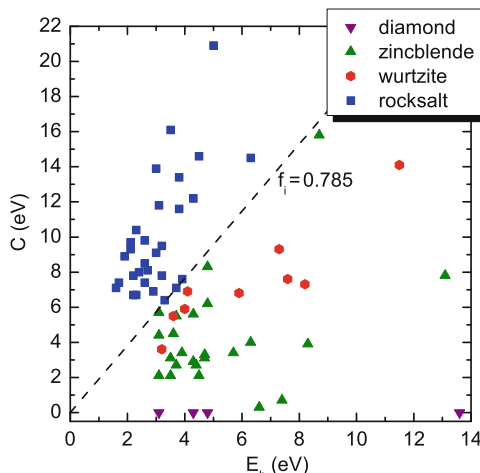
⁴This energy should not be confused with the *band gap* ΔE_{cv} , the energy separation of the highest valence-band state and the lowest conduction-band state. The energy splitting E_{ba} is the energy separation between the centers of the valence and conduction bands. Mostly, the term E_g is used for ΔE_{cv} .

Table 2.1. Ionicity f_i (2.10) for various binary compounds

C	0.0	AlAs	0.27	BeO	0.60	CuCl	0.75
Si	0.0	BeS	0.29	ZnTe	0.61	CuF	0.77
Ge	0.0	AlP	0.31	ZnO	0.62	AgI	0.77
Sn	0.0	GaAs	0.31	ZnS	0.62	MgS	0.79
BAs	0.002	InSb	0.32	ZnSe	0.63	MgSe	0.79
BP	0.006	GaP	0.33	HgTe	0.65	CdO	0.79
BeTe	0.17	InAs	0.36	HgSe	0.68	HgS	0.79
SiC	0.18	InP	0.42	CdS	0.69	MgO	0.84
AlSb	0.25	AlN	0.45	CuI	0.69	AgBr	0.85
BN	0.26	GaN	0.50	CdSe	0.70	LiF	0.92
GaSb	0.26	MgTe	0.55	CdTe	0.72	NaCl	0.94
BeSe	0.26	InN	0.58	CuBr	0.74	RbF	0.96

$$e^*(b) = e^*(b_0) \left(\frac{b}{b_0} \right)^s \approx e_0^* (1 + s\epsilon), \quad (2.11)$$

ϵ being the strain of the bond length, $b/b_0 = 1 + \epsilon$. It seems justified to assume that $e^*(b_0)$ is always positive at the metal atom in III-V and II-VI compounds. The relation of s with the ionicity f_i is shown in Fig. 2.15 for various compound semiconductors.



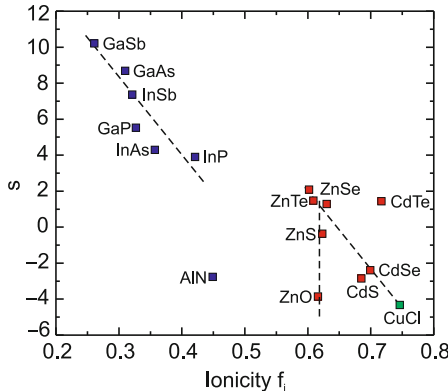


Fig. 2.15. s -Parameter as defined in (2.11) as a function of the ionicity f_i (2.10) for various compound semiconductors. *Dashed lines* are guides to the eye. Data from [111], value for CuCl from [110]

2.5 Metallic Bonding

In a metal, the positively charged atomic cores are embedded in a more or less homogeneous sea of electrons. The valence electrons of the atoms become the conduction electrons of the metal. These are freely moveable and at $T = 0\text{ K}$ there is no energy gap between filled and empty states. The bonding is mediated by the energy reduction for the conduction electrons in the periodic potential of the solid compared to free atoms. This will be clearer when the band structure is discussed (Chap. 6). In transition metals the overlap of inner shells (d or f) can also contribute to the bonding.

2.6 van-der-Waals Bonds

The van-der-Waals bond is a dipole bond that leads to bonding in the noble-gas crystals (at low temperature). Ne, Ar, Kr and Xe crystallize in the densely packed fcc lattice (cf. Sect. 3.3.5). He³ and He⁴ represent an exception. They do not solidify at zero pressure at $T = 0\text{ K}$ due to the large zero-point energy. This quantum-mechanical effect is especially strong for oscillators with small mass.

When two neutral atoms come near to each other (distance of the nuclei R), an attractive dipole–dipole interaction $-AR^{-6}$ arises (London interaction) the van-der-Waals interaction. The quantum-mechanical overlap of the (filled) shells leads to a strong repulsion $+BR^{-12}$. Altogether, a binding energy minimum results for the Lennard–Jones potential V_{LJ} (see Fig. 2.16)

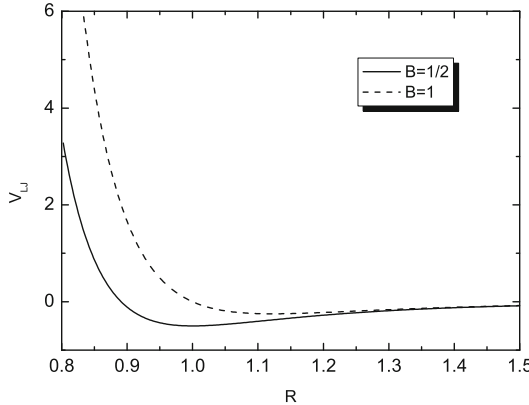


Fig. 2.16. Lennard-Jones potential (2.12) for $A = 1$ and two values of B

$$V_{\text{LJ}}(R) = -\frac{A}{R^6} + \frac{B}{R^{12}} . \quad (2.12)$$

The energy minimum $E_{\min} = -A^2/(2B)$ is at $R = (2B/A)^{1/6}$.

The origin of the attractive dipole-dipole interaction can be understood from a one-dimensional (1D) model as follows: Two atoms are modeled by their fixed positively charged nuclei in a distance R and their negatively charged electron shells that are polarizable, i.e. can be displaced along one direction x . Additionally, we assume (two identical) 1D harmonic oscillators for the electron motion at the positions 0 and R . Then, the Hamilton operator H_0 of the system without interaction (R is very large)

$$H_0 = \frac{1}{2m} p_1^2 + C x_1^2 + \frac{1}{2m} p_2^2 + C x_2^2 . \quad (2.13)$$

The indices 1 and 2 denote the two electrons of atoms. x_1 and x_2 are the displacements of the electrons. Both harmonic oscillators have a resonance frequency $\omega_0 = \sqrt{C/m}$, and the zero-point energy is $\hbar\omega_0/2$.

Taking into account the Coulomb interaction of the four charges, an additional term H_1 arises

$$H_1 = \frac{e^2}{R} + \frac{e^2}{R + x_1 + x_2} - \frac{e^2}{R + x_1} - \frac{e^2}{R - x_2} \approx -\frac{2e^2}{R^3} x_1 x_2 . \quad (2.14)$$

The approximation is valid for small amplitudes $x_i \ll R$. A separation of variables can be achieved by transformation to the normal modes

$$x_s = \frac{x_1 + x_2}{\sqrt{2}}, x_a = \frac{x_1 - x_2}{\sqrt{2}} . \quad (2.15)$$

Then we find

$$\begin{aligned} H &= H_0 + H_1 \\ &= \left[\frac{1}{2m} p_s^2 + \frac{1}{2} \left(C - \frac{2e^2}{R^3} \right) x_s^2 \right] + \left[\frac{1}{2m} p_a^2 + \frac{1}{2} \left(C - \frac{2e^2}{R^3} \right) x_a^2 \right]. \end{aligned} \quad (2.16)$$

This equation is the Hamiltonian of two decoupled harmonic oscillators with the normal frequencies

$$\omega_{\pm} = \sqrt{\left(C \pm \frac{2e^2}{R^3} \right) / m} \approx \omega_0 \left[1 \pm \frac{1}{2} \left(\frac{2e^2}{CR^3} \right) - \frac{1}{8} \left(\frac{2e^2}{CR^3} \right)^2 + \dots \right]. \quad (2.17)$$

The coupled system thus has a lower (zero-point) energy than the uncoupled. The energy difference per atom is (in lowest order) proportional to R^{-6} .

$$\Delta U = \hbar\omega_0 - \frac{1}{2} (\omega_+ - \omega_-) \approx -\hbar\omega_0 \frac{1}{8} \left(\frac{2e^2}{CR^3} \right)^2 = -\frac{A}{R^6}. \quad (2.18)$$

The interaction is a true quantum-mechanical effect, i.e. the reduction of the zero-point energy of coupled oscillators.

2.7 Hamilton Operator of the Solid

The total energy of the solid, including kinetic and potential terms, is

$$\begin{aligned} H = & \sum_i \frac{\mathbf{p}_i^2}{2m_i} + \sum_j \frac{\mathbf{P}_j^2}{2M_j} \\ & + \frac{1}{2} \sum_{j,j'} \frac{Z_j Z_{j'} e^2}{4\pi\epsilon_0 |\mathbf{R}_j - \mathbf{R}_{j'}|} + \frac{1}{2} \sum_{i,i'} \frac{e^2}{4\pi\epsilon_0 |\mathbf{r}_i - \mathbf{r}_{i'}|} \\ & - \sum_{i,j} \frac{Z_j e^2}{4\pi\epsilon_0 |\mathbf{R}_j - \mathbf{r}_i|}, \end{aligned} \quad (2.19)$$

where \mathbf{r}_i and \mathbf{R}_i are the position operators and \mathbf{p}_i and \mathbf{P}_i are the momentum operators of the electrons and nuclei, respectively. The first term is the kinetic energy of the electrons, the second term is the kinetic energy of the nuclei. The third term is the electrostatic interaction of the nuclei, the fourth term is the electrostatic interaction of the electrons. In the third and fourth terms the summation over the same indices is left out. The fifth term is the electrostatic interactions of electrons and nuclei.

In the following, the usual approximations in order to treat (2.19) are discussed. First, the nuclei and the electrons tightly bound to the nuclei

(inner shells) are united with ion cores. The remaining electrons are the valence electrons.

The next approximation is the Born–Oppenheimer (or adiabatic) approximation. Since the ion cores are much heavier than the electrons (factor $\approx 10^3$) they move much slower. The frequencies of the ion vibrations are typically in the region of several tens of meV (phonons, cf. Sect. 5.2), the energy to excite an electron is typically 1 eV. Thus, the electrons always ‘see’ the momentary position of the ions, the ions, however, ‘see’ the electron motions averaged over many periods. Thus, the Hamiltonian (2.19) is split into three parts:

$$H = H_{\text{ions}}(\mathbf{R}_j) + H_e(\mathbf{r}_i, \mathbf{R}_{j_0}) + H_{e-\text{ion}}(\mathbf{r}_i, \delta\mathbf{R}_j) . \quad (2.20)$$

The first term contains the ion cores with their potential and the time-averaged contribution of the electrons. The second term is the electron motion around the ion cores at their averaged positions \mathbf{R}_{j_0} . The third term is the Hamiltonian of the electron–phonon interaction that depends on the electron positions and the deviation of the ions from their average position $\delta\mathbf{R}_j = \mathbf{R}_j - \mathbf{R}_{j_0}$. The electron–phonon interaction is responsible for such effects as electrical resistance and superconductivity.